robotics

MDPI

Article

Instantaneous Kinematics and Free-from-Singularity Workspace of 3-XXRRU Parallel Manipulators

Henrique Simas [1], Raffaele Di Gregorio [2,*] and Roberto Simoni [3]

[1] Raul Guenther Laboratory of Applied Robotics, Department of Mechanical Engineering, Federal University of Santa Catarina, Florianópolis 88040-900, SC, Brazil; henrique.simas@ufsc.br
[2] Laboratory of Mechatronics and Virtual Prototyping (LaMaViP), Department of Engineering, University of Ferrara, Via Saragat, 1, 44100 Ferrara, Italy
[3] Department of Mobility Engineering, Federal University of Santa Catarina, Joinville 89219-600, SC, Brazil; roberto.simoni@ufsc.br
* Correspondence: raffaele.digregorio@unife.it

Abstract: 3-XXRRU parallel manipulators (PMs) constitute a family of six-degrees-of-freedom (DOF) PMs with three limbs of type XXRRU, where R and U stand for revolute pair and universal joint, respectively, and XX indicates any actuated two-DOF mechanism that moves the axis of the first R-pair. The members of this family share the fact that they all become particular 3-RRU structures when the actuators are locked. By exploiting this feature, the present paper proposes a general approach, which holds for all the members of this family, to analyze the instantaneous kinematics, workspace, and kinetostatic performances of any 3-XXRRU PM. The results of this study include the identification of singularity conditions without reference to a specific actuation system, the proposal of two specific dimensionless performance indices ranging from 0 to 1, the determination of the optimal actuation system, and the demonstration that 3-XXRRU PMs, when appropriately sized and actuated, possess a broad singularity-free workspace that is also fully isotropic. These findings hold significance in the context of the dimensional synthesis and control of 3-XXRRU PMs. Moreover, when combined with the closed-form solutions for their positional analysis, as demonstrated in a previous publication by the same authors, 3-XXRRU PMs emerge as intriguing alternatives to other six-DOF PMs. The efficacy of the proposed approach is further illustrated through a case study.

Keywords: parallel manipulators; instantaneous kinematics; singularity analysis; workspace; motion control

Citation: Simas, H.; Di Gregorio, R.; Simoni, R. Instantaneous Kinematics and Free-from-Singularity Workspace of 3-XXRRU Parallel Manipulators. *Robotics* **2023**, *12*, 138. https://doi.org/10.3390/robotics12050138

Academic Editor: Marco Ceccarelli

Received: 30 June 2023
Revised: 27 September 2023
Accepted: 3 October 2023
Published: 5 October 2023

1. Introduction

Parallel manipulators (PMs) [1] feature an end effector (platform) connected to a frame (base) by means of a number of kinematic chains (limbs) that can be of any type (i.e., either open or closed or even hybrid chains). The multiple connections between the platform and base make PMs stiffer and more precise than their serial counterparts but, at the same time, make their kinematics more complex and their workspace smaller.

Usually, the number of limbs is equal to the degrees of freedom (DOF) of the PM, and the limbs are open chains with one actuator per limb, which is located on or near the base to reduce the mobile masses [1–4]. The higher the limb number, the smaller the workspace since the number of possible limb collisions increases. Thus, reducing the limb number without changing the DOF number and actuators' locations is of interest. Such a goal is reachable by using hybrid chains as limbs where more than one actuator per limb, located on the base, controls as many joint variables through a suitable closed-chain transmission. In the literature, a number of six-DOF PMs with only three limbs and more than one actuator per limb have been proposed (see [5–14], for instance).

In this context, the authors of the present paper together with Meneghini [15] have proposed a family of six-DOF PMs with three limbs of XXRRU type[1], where R and U stand for revolute pair and universal joint, respectively, and XX indicates any actuated two-DOF mechanism that moves the axis of the first R-pair. In addition, they have shown that both the direct and the inverse position analyses of 3-XXRRU PMs are solvable in closed form.

The presence of singularities [16–22] can further reduce PMs' useful workspace. By considering the relationship between actuated-joint rates (inputs) and platform twist (output) as an input–output relationship (hereafter named IOR) [16–20], singularities are mechanism configurations where the one-to-one correspondence, which the IOR[2] states, between actuated-joint rates and platform twist fails. With reference to the IOR, two instantaneous kinematics problems are definable: the instantaneous inverse kinematics (IIK) problem, which is the determination of one set of actuated-joint rates compatible with one assigned platform twist, and the instantaneous forward kinematics (IFK) problem, which is the determination of one platform twist compatible with one assigned set of actuated-joint rates. Accordingly, three main types of singularities are identifiable [16]: (I) serial singularities, which are mechanism configurations where the IIK is unsolvable, (II) parallel singularities, which are mechanism configurations where the IFK is unsolvable, and (III) the mechanism configurations where both the problems are unsolvable.

Serial singularities are by definition configurations from which the platform cannot exit by moving along any direction (twist), that is, there is a local reduction in the platform's DOF number. Such a condition occurs at the workspace boundaries. Differently, parallel singularities are by definition configurations where the actuated joints are not enough to fully control the platform twist, that is, somehow, there is a local increase in the platform's DOF number. This condition can occur only in PMs and, unfortunately, it usually occurs inside the workspace. The duality, the virtual work principle states between instantaneous kinematics and statics, brings one to conclude that, at a parallel singularity, a small load (even elementary) applied to the platform needs infinite generalized torques at least in one actuator to be equilibrated. Moreover, the nearer the PM configuration to a parallel singularity, the higher the internal loads in the links and the generalized torques in the actuators. In short, a PM must stay far enough from parallel singularities to avoid its breakdown. That is the reason why parallel singularities must be identified during PMs' design and must be avoided during functioning. Therefore, the existence of parallel singularities constitutes a further limitation to the useful workspace of a PM, which might be even tighter than the one due to there being a high number of limbs.

The 3-XXRRU PMs, as proposed in [15], all share a common characteristic: when the actuators are locked, they all transform into specific 3-RRU structures (refer to Figure 1). In each RRU limb of these structures, the axes of the first three R-pairs are parallel, while the axis of the fourth R-pair (i.e., the one fixed to the platform) is perpendicular to the axes of all the other R-pairs[3]. Leveraging this characteristic, this paper presents a general approach applicable to all such PMs. This approach is used to analyze the instantaneous kinematics, workspace, and kinetostatic performance of any 3-XXRRU PM.

The key findings of this study are as follows:

(i) Identification of singularity conditions without the need to reference a specific actuation system;
(ii) Introduction of two dimensionless performance indices ranging from 0 to 1;
(iii) Determination of the optimal actuation system;

[1] The sequence of capital letters indicates the types of joints or sub-mechanisms encountered by moving from the base to the platform along the limb.

[2] It is worth noting that the input–output instantaneous relationship (IOR) of manipulators is always linear and homogeneous both in the actuated-joint rates (inputs) and in the platform twist (output) [16,18] since it is the time derivative of the mechanism constraint-equation system which is holonomic and time independent for manipulators.

[3] It is worth noting that a U joint consists of two R-pairs in series with mutually orthogonal axes, which intersect one another at a point, named the center of the U joint.

(iv) Demonstration that suitably sized and actuated 3-XXRRU PMs offer a broad, singularity-free workspace that is fully isotropic.

These results hold significant relevance for the dimensional synthesis and control of 3-XXRRU PMs. Moreover, the availability of closed-form solutions for their position analysis problems positions 3-XXRRU PMs as intriguing alternatives to other six-DOF PMs. The effectiveness of the proposed approach is further illustrated through a case study.

The paper is organized as follows. Section 2 provides the necessary background materials on 3-XXRRU PMs, deduces their IOR for a general geometry, and presents their singularity analysis together with how to evaluate their kinetostatic performances. Then, Section 3 applies the found singularity conditions and performance indices to a case study, and Section 4 discusses the results. Finally, Section 5 draws the conclusions.

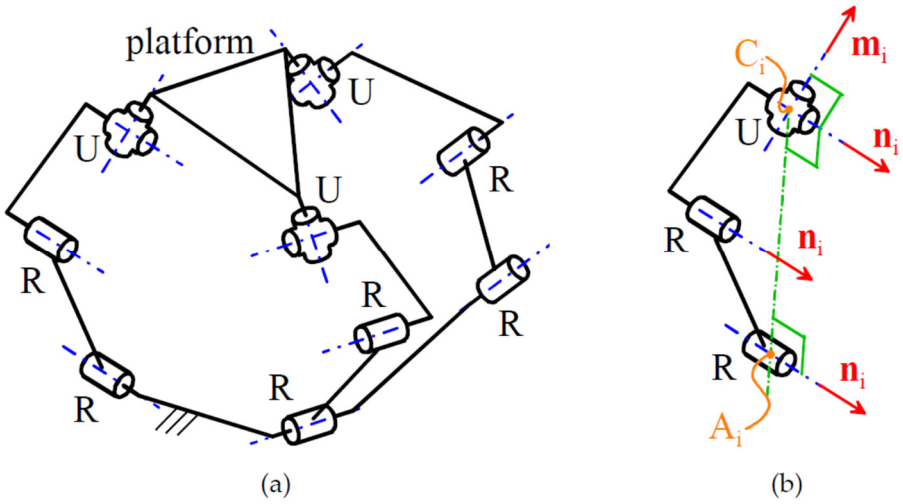

Figure 1. Notations: (**a**) a 3-RRU structure generated from a 3-XXRRU PM by locking the actuators and (**b**) the *i*-th RRU limb, for $i = 1, 2, 3$, of the 3-RRU structure.

2. Materials and Methods

By considering each limb of a PM as a unique articulated joint whose DOF number is equal to the limb connectivity[4] [21–23], the *general mobility criterion*[5] [21,22] brings one to conclude that adding any number of limbs with connectivity equal to six does not reduce the mobility of the platform with respect to the base (i.e., the resulting PM architecture always has six DOFs). Limbs of XXRRU type have connectivity equal to six when the two DOFs provided by the XX mechanism do not replicate any DOF provided by the remaining RRU kinematic chain. In particular, the first three R-pairs of the RRU chain (Figure 1b), which have parallel axes, generate a planar motion with a motion plane perpendicular to the axes of these R-pairs. Then, the fourth R-pair of the RRU chain (i.e., the one adjacent to the platform) adds a rotation around an axis that is parallel to the above-said motion plane. Therefore, in order to make the platform motion a general six-DOF motion through an XXRRU limb, the further two DOFs of the XX mechanism must provide either a general reorientation of the above-said motion plane (i.e., a general change in the direction of the axes of the first three R-pairs) or a translation perpendicular to the above-mentioned motion plane together with a particular reorientation of the same plane that involves only one DOF. If these conditions are respected in all three XXRRU limbs, the resulting 3-XXRRU PM will have six DOFs.

[4] The connectivity of a limb is by definition the DOF number of the kinematic chain constituted by platform and base uniquely connected by that limb.

[5] Such a criterion counts the DOF number, l, of a spatial mechanism through the formula $l = 6(m-1) - \sum_{i=1,6}(6-i)c_i$ where m is the number of rigid bodies and c_i is the number of constraints with i DOF among the m bodies.

When the actuators are locked, all of the 3-XXRRU PMs, presented in [15], become 3-RRU structures (Figure 1). In the *i*-th RRU limb (Figure 1b), for i = 1, 2, 3, the axis, (A_i, $\mathbf{n}_i$)[6], of the first R-pair is located through the coordinates of a point, A_i, belonging to it, and a unit vector, $\mathbf{n}_i$, parallel to it. The axis, (C_i, $\mathbf{m}_i$), of the fourth R-pair, fixed to the platform, is located through the coordinates of the center, C_i, of the U joint and a unit vector, $\mathbf{m}_i$, parallel to it. Without losing generality, point A_i is chosen lying on the plane perpendicular to $\mathbf{n}_i$ that passes through C_i.

With these notations, the actuated two-DOF mechanism, XX, of the *i*-th limb may change only two parameters chosen among the A_i coordinates and/or the $\mathbf{n}_i$ components by respecting the above-defined mobility conditions. Moreover, parallel singularities of 3-XXRRU PMs correspond to configurations of the 3-RRU sub-structure at which the platform can perform elementary motions.

2.1. Input–Output Instantaneous Relationship

The IOR of any 3-XXRRU PM of this family is deducible by time differentiating its constraint equation system, which is writable as follows (see Figure 1b; hereafter, a bold letter denotes a vector and a bold capital letter referable to a point denotes the position vector of that point measured in a reference system fixed to the base):

$$(\mathbf{C}_i - \mathbf{A}_i) \cdot \mathbf{n}_i = 0 \qquad i = 1, 2, 3 \tag{1a}$$

$$\mathbf{m}_i \cdot \mathbf{n}_i = 0 \qquad i = 1, 2, 3 \tag{1b}$$

The time derivative of system (1) is:

$$\dot{\mathbf{C}}_i \cdot \mathbf{n}_i = \dot{\mathbf{A}}_i \cdot \mathbf{n}_i + (\mathbf{A}_i - \mathbf{C}_i) \cdot \dot{\mathbf{n}}_i \qquad i = 1, 2, 3 \tag{2a}$$

$$\dot{\mathbf{m}}_i \cdot \mathbf{n}_i = -\mathbf{m}_i \cdot \dot{\mathbf{n}}_i \qquad i = 1, 2, 3 \tag{2b}$$

Let P and $\boldsymbol{\omega}$ be a point fixed to the platform and the angular velocity of the platform, respectively. Since points C_i and unit vectors $\mathbf{m}_i$, for i = 1, 2, 3, are fixed to the platform, the following relationships of rigid-body mechanics hold [23]:

$$\dot{\mathbf{C}}_i = \dot{\mathbf{P}} + \boldsymbol{\omega} \times (\mathbf{C}_i - \mathbf{P}) \quad i = 1, 2, 3 \tag{3a}$$

$$\dot{\mathbf{m}}_i = \boldsymbol{\omega} \times \mathbf{m}_i \quad i = 1, 2, 3 \tag{3b}$$

whose introduction into Equations (2a) and (2b), after some simple rearrangements that use the properties of the mixed product of three vectors, yields:

$$\mathbf{n}_i \cdot \dot{\mathbf{P}} + [(\mathbf{C}_i - \mathbf{P}) \times \mathbf{n}_i] \cdot \boldsymbol{\omega} = \mathbf{n}_i \cdot \dot{\mathbf{A}}_i + (\mathbf{A}_i - \mathbf{C}_i) \cdot \dot{\mathbf{n}}_i \quad i = 1, 2, 3 \tag{4a}$$

$$(\mathbf{n}_i \times \mathbf{m}_i) \cdot \boldsymbol{\omega} = \mathbf{m}_i \cdot \dot{\mathbf{n}}_i \quad i = 1, 2, 3 \tag{4b}$$

[6] Hereafter, a line will be denoted (P, **u**) where P is a point belonging to the line and u is a unit vector parallel to the line.

Equations (4a) and (4b) are writable in matrix form as follows:

$$\begin{bmatrix} \mathbf{N}^T & \mathbf{H}^T \\ \mathbf{0}_{3\times3} & \mathbf{M}^T \end{bmatrix} \begin{pmatrix} \dot{\mathbf{P}} \\ \boldsymbol{\omega} \end{pmatrix} = \begin{pmatrix} \mathbf{n}_1 \cdot \dot{\mathbf{A}}_1 + (\mathbf{A}_1 - \mathbf{C}_1) \cdot \dot{\mathbf{n}}_1 \\ \mathbf{n}_2 \cdot \dot{\mathbf{A}}_2 + (\mathbf{A}_2 - \mathbf{C}_2) \cdot \dot{\mathbf{n}}_2 \\ \mathbf{n}_3 \cdot \dot{\mathbf{A}}_3 + (\mathbf{A}_3 - \mathbf{C}_3) \cdot \dot{\mathbf{n}}_3 \\ \mathbf{m}_1 \cdot \dot{\mathbf{n}}_1 \\ \mathbf{m}_2 \cdot \dot{\mathbf{n}}_2 \\ \mathbf{m}_3 \cdot \dot{\mathbf{n}}_3 \end{pmatrix} \tag{5}$$

where $\mathbf{0}_{3\times3}$ is the 3×3 null matrix and $\hat{\$} = \begin{pmatrix} \dot{\mathbf{P}} \\ \boldsymbol{\omega} \end{pmatrix}$ is the platform twist; whereas $\mathbf{N}$, $\mathbf{M}$, and $\mathbf{H}$ are 3×3 matrices defined as follows:

$$\mathbf{N} = \begin{bmatrix} \mathbf{n}_1 & \mathbf{n}_2 & \mathbf{n}_3 \end{bmatrix}, \ \mathbf{M} = \begin{bmatrix} (\mathbf{n}_1 \times \mathbf{m}_1) & (\mathbf{n}_2 \times \mathbf{m}_2) & (\mathbf{n}_3 \times \mathbf{m}_3) \end{bmatrix}, \tag{6a}$$

$$\mathbf{H} = \begin{bmatrix} (\mathbf{C}_1 - \mathbf{P}) \times \mathbf{n}_1 & (\mathbf{C}_2 - \mathbf{P}) \times \mathbf{n}_2 & (\mathbf{C}_3 - \mathbf{P}) \times \mathbf{n}_3 \end{bmatrix}; \tag{6b}$$

In system (5), $\dot{\mathbf{A}}_i$ and $\dot{\mathbf{n}}_i$, for i = 1, 2, 3, are linearly related to the actuated-joint rates through linear and homogeneous expressions that depend on the type of two-DOF mechanism XX, which is present in the XXRRU limb. System (5) is the IOR of a generic 3-XXRRU PM.

2.2. Singularity Analysis

The singularity analysis, which is the determination of the geometric/analytic conditions that identify the singular configurations (singularities), practically consists of analyzing the IOR of the PM, that is, system (5) for a 3-XXRRU PM.

Regarding the possible actuation choices for these PMs, system (5) immediately reveals that, if the XX mechanisms only move points A_i, for i = 1, 2, 3, (i.e., $\dot{\mathbf{n}}_1 = \dot{\mathbf{n}}_2 = \dot{\mathbf{n}}_3 = 0$), the last three equations, which simply become $\mathbf{M}^T \boldsymbol{\omega} = \mathbf{0}$, always provide $\boldsymbol{\omega} = \mathbf{0}$ out of singularities that make det($\mathbf{M}$) = 0. That is, with this actuation choice, the platform can only translate and the 3-XXRRU becomes a 3-DOF translational PM (TPM). The so-obtained TPM is somehow a more general geometry of the Cartesian TPM proposed by Kim and Tsai in [24,25]. Moreover, since $\dot{\mathbf{A}}_i$ only appears in the dot product $\mathbf{n}_i \cdot \dot{\mathbf{A}}_i$, the only motion direction of point A_i that causes a platform motion is the one along $\mathbf{n}_i$. In particular, since the time derivative of $\mathbf{n}_i \cdot \mathbf{n}_i = 1$ yields $\mathbf{n}_i \cdot \dot{\mathbf{n}}_i = 0$, choosing $\dot{\mathbf{A}}_i = a_i \dot{\mathbf{n}}_i$ where a_i is an arbitrary scalar constant would give $\mathbf{n}_i \cdot \dot{\mathbf{A}}_i = a_i \mathbf{n}_i \cdot \dot{\mathbf{n}}_i = 0$, that is, no effect on the platform motion. In short, the XX mechanism of the i-th XXRRU limb can devote at most one actuator to move point A_i and must move it only along $\mathbf{n}_i$, and an actuated prismatic (P) pair with sliding direction parallel to $\mathbf{n}_i$ that moves point A_i does not affect the platform translation through the term $\mathbf{n}_i \cdot \dot{\mathbf{A}}_i$ when the direction of $\mathbf{n}_i$ changes and the P pair is locked.

Differently, the same analysis, reveals that if the XX mechanisms only change the directions of unit vectors $\mathbf{n}_i$, for i = 1, 2, 3, (i.e., $\dot{\mathbf{A}}_1 = \dot{\mathbf{A}}_2 = \dot{\mathbf{A}}_3 = 0$), the platform can perform a general 6-DOF motion since $\dot{\mathbf{n}}_i$, for i = 1, 2, 3, appears in all six equations of system (5). In particular, since, in the last three equations of system (5), $\dot{\mathbf{n}}_i$ appears only in the dot product $\mathbf{m}_i \cdot \dot{\mathbf{n}}_i$, the component of $\dot{\mathbf{n}}_i$ that makes the platform orientation change is only the one along the direction of $\mathbf{m}_i$. Moreover, since, in the first three equations of system (5), $\dot{\mathbf{n}}_i$ appears only in the dot product $(\mathbf{A}_i - \mathbf{C}_i) \cdot \dot{\mathbf{n}}_i$, the component of $\dot{\mathbf{n}}_i$ that makes the platform translate is only the one along the direction of $(\mathbf{A}_i - \mathbf{C}_i)$.

The conclusion is that the most effective actuation system is a two-DOF mechanism that, firstly, controls the $\mathbf{n}_i$ direction and then, after having obtained the desired platform orientation, locks the $\mathbf{n}_i$ direction through a system of clutches and brakes, and, eventually,

uses one of the two actuators previously used to change the $\mathbf{n}_i$ direction to make the platform translate toward the desired final pose by moving A_i along the $\mathbf{n}_i$ direction.

The above discussion of the possible actuation choices makes clear that when one entry of the six-tuple that appears on the right-hand side of system (5) is equal to zero, even though $\dot{\mathbf{A}}_i$ and/or $\dot{\mathbf{n}}_i$ are different from zero, some of the actuated-joint rates are indeterminate for an assigned platform twist, that is, a serial singularity occurs. Therefore, from an analytical point of view, a serial singularity occurs when, provided that $\dot{\mathbf{A}}_i$ and/or $\dot{\mathbf{n}}_i$ are different from zero, at least one of the following six conditions is satisfied:

$$\mathbf{n}_i \cdot \dot{\mathbf{A}}_i + (\mathbf{A}_i - \mathbf{C}_i) \cdot \dot{\mathbf{n}}_i = 0 \qquad i = 1, 2, 3 \tag{7a}$$

$$\mathbf{m}_i \cdot \dot{\mathbf{n}}_i = 0 \qquad i = 1, 2, 3 \tag{7b}$$

Differently, a parallel singularity occurs when the six-tuple on the right-hand side of system (5) is assigned, but the corresponding platform twist is not computable by solving system (5). This can happen if and only if the determinant of the 6×6 matrix (parallel Jacobian) that multiplies the platform twist on the left-hand side of system (5) is equal to zero. Since this parallel Jacobian is an upper triangular block matrix, the following relationship holds [26,27]:

$$\det\begin{pmatrix} \mathbf{N}^T & \mathbf{H}^T \\ \mathbf{0}_{3\times 3} & \mathbf{M}^T \end{pmatrix} = \det(\mathbf{N})\det(\mathbf{M}) \tag{8}$$

where, by remembering definition (6a), the following geometric/analytic explicit expressions of $\det(\mathbf{N})$ and $\det(\mathbf{M})$ can be introduced:

$$\det(\mathbf{N}) = \mathbf{n}_1 \cdot (\mathbf{n}_2 \times \mathbf{n}_3), \ \det(\mathbf{M}) = (\mathbf{n}_1 \times \mathbf{m}_1) \cdot [(\mathbf{n}_2 \times \mathbf{m}_2) \times (\mathbf{n}_3 \times \mathbf{m}_3)]. \tag{9}$$

Therefore, a parallel singularity occurs if and only if one or the other of the following two conditions is satisfied:

$$\mathbf{n}_1 \cdot (\mathbf{n}_2 \times \mathbf{n}_3) = 0, \tag{10a}$$

$$(\mathbf{n}_1 \times \mathbf{m}_1) \cdot [(\mathbf{n}_2 \times \mathbf{m}_2) \times (\mathbf{n}_3 \times \mathbf{m}_3)] = 0 \tag{10b}$$

Since the left-hand sides of both Equations (10a) and (10b) are mixed products of unit vectors, Equation (10a) (Equation (10b)) is satisfied if and only if the three unit vectors $\mathbf{n}_i$, for i = 1, 2, 3, (the three unit vectors $\mathbf{n}_i \times \mathbf{m}_i$, for i = 1, 2, 3) are all parallel to a unique plane. From a kinematic point of view, the analysis of system (5) reveals that, when Equation (10a) (Equation (10b)) is satisfied, even though the actuated joints are locked, that is, even though $\dot{\mathbf{A}}_i = 0$ and $\dot{\mathbf{n}}_i = 0$ for i = 1, 2, 3, $\dot{\mathbf{P}}$ ($\boldsymbol{\omega}$) has an indeterminate component along the direction perpendicular to the unique plane the three unit vectors $\mathbf{n}_i$, for i = 1, 2, 3, (the three unit vectors $\mathbf{n}_i \times \mathbf{m}_i$, for i = 1, 2, 3) are parallel to, that is, the platform can translate along (rotate around a line parallel to) that direction.

2.3. Evaluation of Kinetostatic Performance

From a geometric point of view, the absolute value of the mixed product of three unit vectors, $\mathbf{u}_i$, for i = 1, 2, 3, where $\mathbf{u}_i$ can be either $\mathbf{n}_i$ or $\mathbf{n}_i \times \mathbf{m}_i$, is equal to the volume of the rhombohedron (Figure 2) whose three non-parallel edges are parallel to the three unit vectors $\mathbf{u}_i$, for i = 1, 2, 3, and have a length equal to one. Such a volume ranges from 0, when the rhombohedron is flattened, to 1, when the rhombohedron is a cube, and, in this case, can be used as an dimensionless index, say j_u ($\equiv |\mathbf{u}_1 \cdot (\mathbf{u}_2 \times \mathbf{u}_3)|$), of the distance of a non-singular configuration from a parallel singularity since the greater the volume is, the further away the configuration is from satisfying Equation (10). Such an index can be

analytically expressed as a function of two angles, $\theta_{1,u}$ and $\theta_{2,u}$ (Figure 2), which range from 0° to 90°, as follows:

$$j_u \equiv |\mathbf{u}_1 \cdot (\mathbf{u}_2 \times \mathbf{u}_3)| \equiv |\lambda_1 \lambda_2 \lambda_3| = \cos\theta_{1,u} \sin\theta_{2,u} \tag{11}$$

where λ_i, for $i = 1, 2, 3$, are the three eigenvalues of matrix $\mathbf{U} = \begin{bmatrix} \mathbf{u}_1 & \mathbf{u}_2 & \mathbf{u}_3 \end{bmatrix}$.

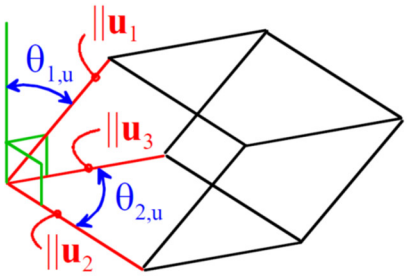

Figure 2. Rhombohedron with an edge length equal to one, which is associated with the three unit vectors $\mathbf{u}_i$, for $i = 1, 2, 3$.

Equations (8), (9) and (11) bring one to build the following index, J, for evaluating the kinetostatic performance of a 3-RRU configuration[7]:

$$J \equiv |\mathbf{n}_1 \cdot (\mathbf{n}_2 \times \mathbf{n}_3)||(\mathbf{n}_1 \times \mathbf{m}_1) \cdot [(\mathbf{n}_2 \times \mathbf{m}_2) \times (\mathbf{n}_3 \times \mathbf{m}_3)]| = j_n j_{n\times m} = \cos\theta_{1,n} \sin\theta_{2,n} \cos\theta_{1,n\times m} \sin\theta_{2,n\times m} \tag{12}$$

From a static point of view (Figure 3), the i-th limb applies to the platform one force, $F_i\mathbf{n}_i$, where F_i is the signed magnitude, parallel to $\mathbf{n}_i$ and with its line of action passing through C_i, and one moment, $M_i(\mathbf{n}_i \times \mathbf{m}_i)$, where M_i is the signed magnitude, parallel to $(\mathbf{n}_i \times \mathbf{m}_i)$. Thus, the equilibrium equations of the platform are ($\mathbf{F}_e$ and $\mathbf{M}_{e,P}$ are the resultant force and the resultant moment about point P of the external force system applied to the platform):

$$\sum_{i=1,3} F_i\mathbf{n}_i + \mathbf{F}_e = \mathbf{0} \tag{13a}$$

$$\sum_{i=1,3} F_i[(\mathbf{C}_i - \mathbf{P}) \times \mathbf{n}_i] + \sum_{i=1,3} M_i(\mathbf{n}_i \times \mathbf{m}_i) + \mathbf{M}_{e,P} = \mathbf{0} \tag{13b}$$

which, in matrix form, become:

$$\begin{bmatrix} \mathbf{N} & \mathbf{0}_{3\times3} \\ \mathbf{H} & \mathbf{M} \end{bmatrix} \begin{pmatrix} F_1 \\ F_2 \\ F_3 \\ M_1 \\ M_2 \\ M_3 \end{pmatrix} = -\begin{pmatrix} \mathbf{F}_e \\ \mathbf{M}_{e,P} \end{pmatrix} \tag{14}$$

The first three equations of system (14) show that when j_n ($\equiv |\mathbf{n}_1 \cdot (\mathbf{n}_2 \times \mathbf{n}_3)|$) is equal to 1 (i.e., matrix $\mathbf{N}$ is isotropic [28]), by changing the direction of $\mathbf{F}_e$, the condition $|F_i| \leq \|\mathbf{F}_e\|$, for $i = 1, 2, 3$, is always satisfied (i.e., no limb must apply a force with a magnitude greater than the one of $\mathbf{F}_e$). Analogously, when a pure moment $\mathbf{M}_{e,P}$ (i.e., $\mathbf{M}_{e,P} \neq 0$ and $\mathbf{F}_e = \mathbf{0}$) is applied to the platform and $j_{n\times m}$ ($\equiv |(\mathbf{n}_1 \times \mathbf{m}_1) \cdot [(\mathbf{n}_2 \times \mathbf{m}_2) \times (\mathbf{n}_3 \times \mathbf{m}_3)]|$) is equal to 1 (i.e., matrix $\mathbf{M}$ is isotropic [28]), the last three equations of system (14) show that, by changing the direction of $\mathbf{M}_{e,P}$, the condition $|M_i| \leq \|\mathbf{M}_{e,P}\|$, for $i = 1, 2, 3$, is always satisfied (i.e., no limb must apply a moment with a magnitude greater than the one of $\mathbf{M}_{e,P}$). Accordingly, hereafter, a 3-RRU configuration with $j_n = 1$ ($j_{n\times m} = 1$) is named

[7] With reference to Figure 1b, it is worth stressing that the positive direction, toward which the unit vectors $\mathbf{n}_i$ and $\mathbf{m}_i$, for $i = 1, 2, 3$, point, is arbitrarily chosen and that it does not affect the values of j_n and $j_{n\times m}$.

isotropic with respect to $\mathbf{F}_e$ ($\mathbf{M}_{e,P}$). Of course, the best redistribution of loads among the limbs occurs at configurations that are isotropic with respect to both $\mathbf{F}_e$ and $\mathbf{M}_{e,P}$, that is, when $J = j_n j_{n\times m} = 1$, hereafter named *fully isotropic*.

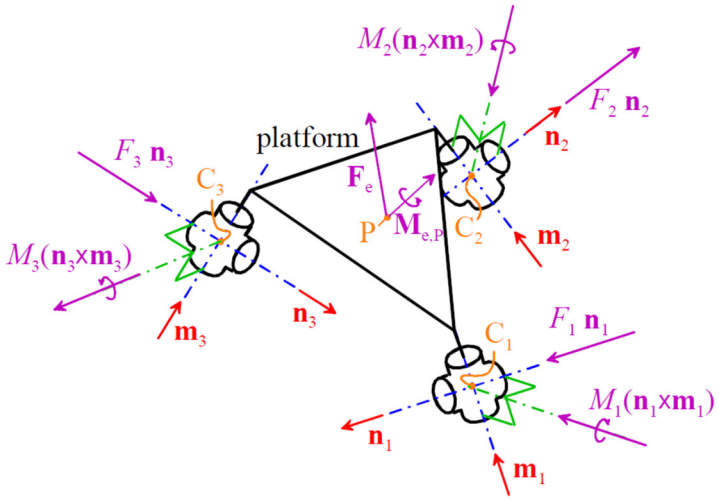

Figure 3. Free-body diagram of the platform.

3. Results

This section proves the effectiveness of the relationships deduced in Section 2 by applying them to the analysis of a 3-XXRRU PM with the geometry shown in Figure 4. In particular, the relationships deduced in Section 2 are used here for the determination of the free-from-singularity workspace of that 3-XXRRU PM and of its kinetostatic performances inside that workspace.

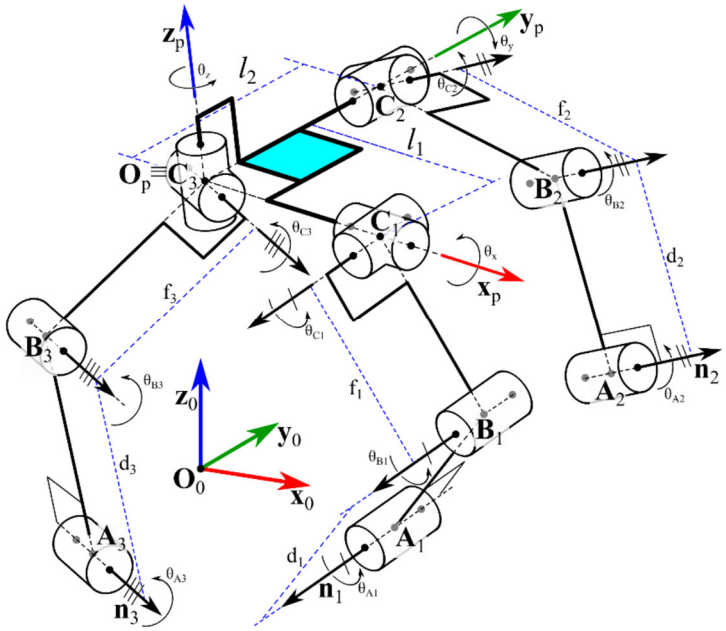

Figure 4. Geometry of the studied 3-XXRRU.

The geometry of the studied 3-XXRRU PM has the peculiarity (see Figure 4) that the axes of the three R-pairs adjacent to the platform share a common intersection, point C_3, and are mutually orthogonal. As a consequence, this particular geometry allows the introduction of a Cartesian reference system $O_p x_p y_p z_p$ (Figure 4), fixed to the platform

with origin, O_p, coincident with C_3 and coordinate axes coincident with the axes of the three R-pairs adjacent to the platform.

With reference to Figure 4 and the general notations of Figure 1, the following further specific notations are introduced. $\mathbf{x}_p$, $\mathbf{y}_p$, and $\mathbf{z}_p$ are the unit vectors of the x_p, y_p, and z_p coordinate axes, respectively, of the $O_p x_p y_p z_p$ reference system and are chosen so that $\mathbf{x}_p \equiv \mathbf{m}_1$, $\mathbf{y}_p \equiv \mathbf{m}_2$, and $\mathbf{z}_p \equiv \mathbf{m}_3$. $O_0 x_0 y_0 z_0$ is a Cartesian reference system fixed to the base. l_1 and l_2 are the lengths of the segments C_3C_1 and C_3C_2. In the i-th limb, for i = 1, 2, 3, point B_i is the intersection of the second R-pair's axis with the plane perpendicular to $\mathbf{n}_i$ and passing through C_i; also, d_i and f_i are the lengths of the segments A_iB_i and B_iC_i, respectively. Moreover, one assumes that the XX mechanism can, firstly, freely orientate unit vector $\mathbf{n}_i$ and then make the platform translate toward the desired final pose, which, as explained in Section 2.2, is the best actuation technique for 3-XXRRU PMs.

Since the actuation system can freely orientate unit vectors $\mathbf{n}_i$, for i = 1, 2, 3, the choice of moving them so that they are always mutually orthogonal is assumed. Such a choice makes all the reached 3-RRU configurations isotropic with respect to $\mathbf{F}_e$ (i.e., with j_n = 1). Therefore, the kinetostatic performance of each 3-RRU configuration could degrade only because of a $j_{n\times m}$ value lower than 1 and can be evaluated by using only the $j_{n\times m}$ index. Nevertheless, for this particular geometry and $\mathbf{n}_i$ motion strategy, the demonstration that follows shows that the index $j_{n\times m}$ is equal to one, too (i.e., the platform moves by keeping the 3-XXRRU configuration fully isotropic). Indeed, with reference to Figure 5, the following explicit expressions can be written.

$$\begin{cases} \mathbf{n}_1 = -\mathbf{m}_2 \sin\theta_x + \mathbf{m}_3 \cos\theta_x \\ \mathbf{n}_2 = \mathbf{m}_1 \sin\theta_y + \mathbf{m}_3 \cos\theta_y \\ \mathbf{n}_3 = -\mathbf{m}_1 \sin\theta_z + \mathbf{m}_2 \cos\theta_z \end{cases} \tag{15a}$$

$$\left.\begin{cases} \mathbf{n}_1 \times \mathbf{m}_1 = \mathbf{m}_3 \sin\theta_x + \mathbf{m}_2 \cos\theta_x \\ \mathbf{n}_2 \times \mathbf{m}_2 = \mathbf{m}_3 \sin\theta_y - \mathbf{m}_1 \cos\theta_y \\ \mathbf{n}_3 \times \mathbf{m}_3 = \mathbf{m}_2 \sin\theta_z + \mathbf{m}_1 \cos\theta_z \end{cases}\right\} \Rightarrow j_{n\times m} = \left|\cos\theta_x \sin\theta_y \cos\theta_z - \sin\theta_x \cos\theta_y \sin\theta_z\right| \tag{15b}$$

Moreover, since unit vectors $\mathbf{n}_i$, for i = 1, 2, 3, are moved by keeping them mutually orthogonal, the following system of three equations in three unknowns must be satisfied

:

$$\begin{cases} \mathbf{n}_1 \cdot \mathbf{n}_2 = (-\mathbf{m}_2 \sin\theta_x + \mathbf{m}_3 \cos\theta_x) \cdot (\mathbf{m}_1 \sin\theta_y + \mathbf{m}_3 \cos\theta_y) = \cos\theta_x \cos\theta_y = 0 \\ \mathbf{n}_1 \cdot \mathbf{n}_3 = (-\mathbf{m}_2 \sin\theta_x + \mathbf{m}_3 \cos\theta_x) \cdot (-\mathbf{m}_1 \sin\theta_z + \mathbf{m}_2 \cos\theta_z) = -\sin\theta_x \cos\theta_z = 0 \\ \mathbf{n}_2 \cdot \mathbf{n}_3 = (\mathbf{m}_1 \sin\theta_y + \mathbf{m}_3 \cos\theta_y) \cdot (-\mathbf{m}_1 \sin\theta_z + \mathbf{m}_2 \cos\theta_z) = -\sin\theta_y \sin\theta_z = 0 \end{cases} \tag{16}$$

whose solutions are ($\cos\theta_x$, $\sin\theta_y$, $\cos\theta_z$) = (0, 0, 0), which implies ($\sin\theta_x$, $\cos\theta_y$, $\sin\theta_z$) = ($\pm$1, $\pm$1, $\pm$1) and ($\sin\theta_x$, $\cos\theta_y$, $\sin\theta_z$) = (0, 0, 0), which implies ($\cos\theta_x$, $\sin\theta_y$, $\cos\theta_z$) = ($\pm$1, $\pm$1, $\pm$1). Both these solutions, when introduced into Equation (15b), yield $j_{n\times m} = 1$, which demonstrates what has been declared above.

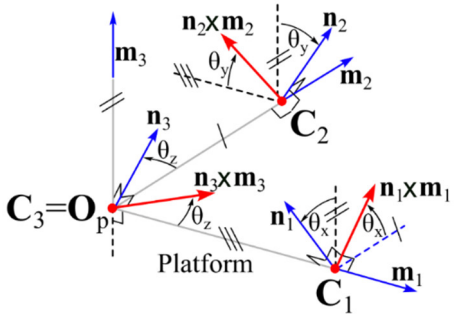

Figure 5. Geometric relationships among the unit vectors $\mathbf{n}_i$, $\mathbf{m}_i$, and $\mathbf{n}_i \times \mathbf{m}_i$, for i = 1, 2, 3, in the platform of the 3-XXRRU shown in Figure 4.

With the above-reported assumptions and choices, the free-from-singularity orientation workspace was numerically determined by using the following data (l.u. stands for arbitrary length unit; the points' coordinates are measured in $O_0x_0y_0z_0$): $A_1 = (1, 1, 0)^T$ l.u., $A_2 = (0, 3, 2)^T$ l.u., $A_3 = (0, 0, 2)^T$ l.u., $l_1 = 1.5$ l.u., $l_2 = 2$ l.u., $d_1 = d_2 = d_3 = 3$ l.u., $f_1 = f_2 = f_3 = 2.5$ l.u. Figure 6 shows the so-determined free-from-singularity orientation workspace (the parameters ϕ_1, ϕ_2, and ϕ_3 on the axes are the ZYZ Euler angles that locate the orientation of $O_px_py_pz_p$ with respect to $O_0x_0y_0z_0$). Figure 7 shows the volume inside which point C_3 moves while the directions of unit vectors $\mathbf{n}_i$, for $i = 1, 2, 3$, are modified (by keeping them mutually orthogonal) to make the platform reach the orientation shown in Figure 6 (the coordinates of point C_3 measured in $O_0x_0y_0z_0$ are reported on the axes of Figure 7).

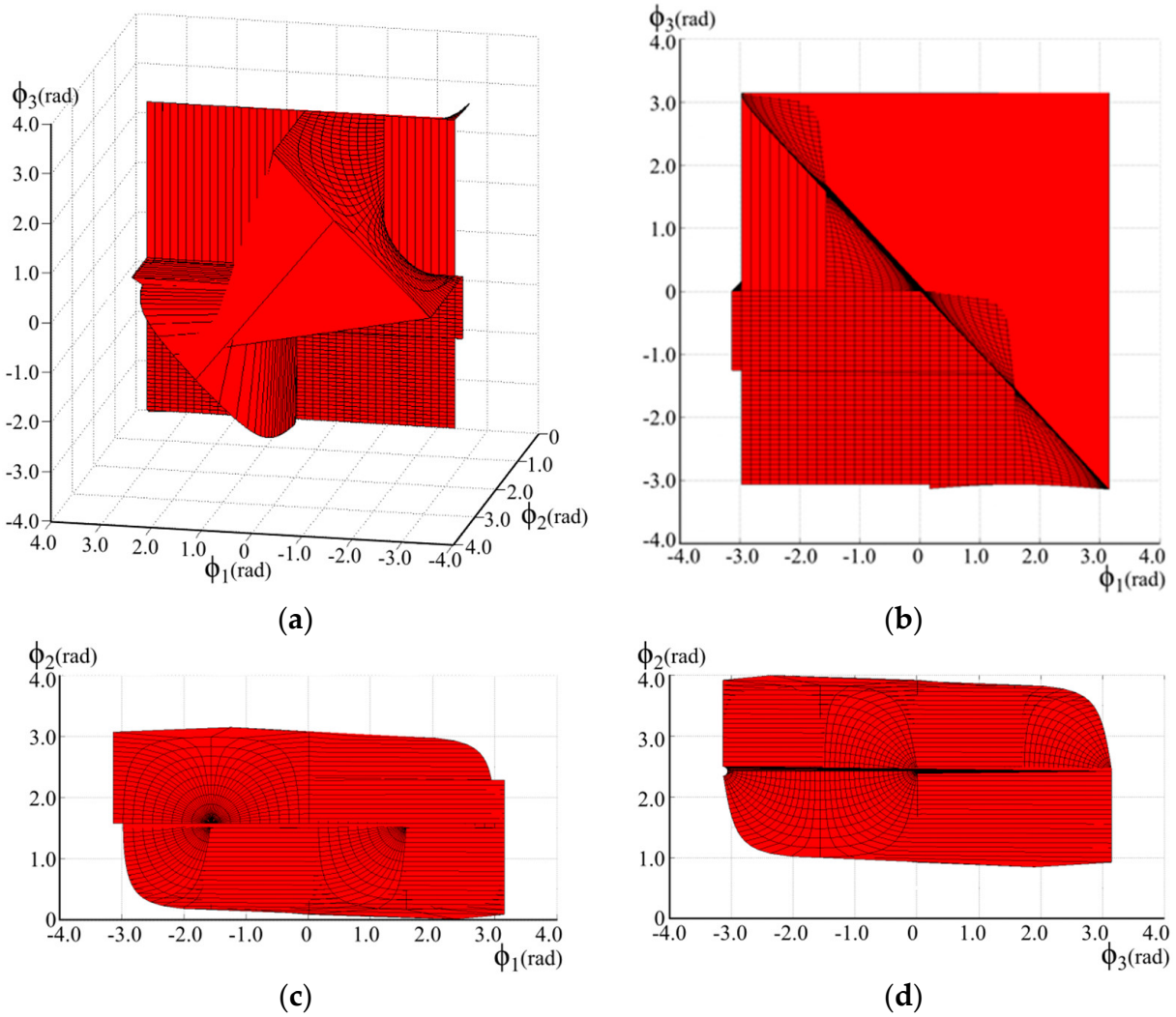

Figure 6. Computed free-from-singularity orientation workspace (the parameters ϕ_1, ϕ_2, and ϕ_3 on the axes are the ZYZ Euler angles that locate the orientation of $O_px_py_pz_p$ with respect to $O_0x_0y_0z_0$): (**a**) 3D view, (**b**) projection onto the $\phi_1\phi_3$-plane, (**c**) projection onto the $\phi_1\phi_2$-plane, and (**d**) projection onto the $\phi_2\phi_3$-plane.

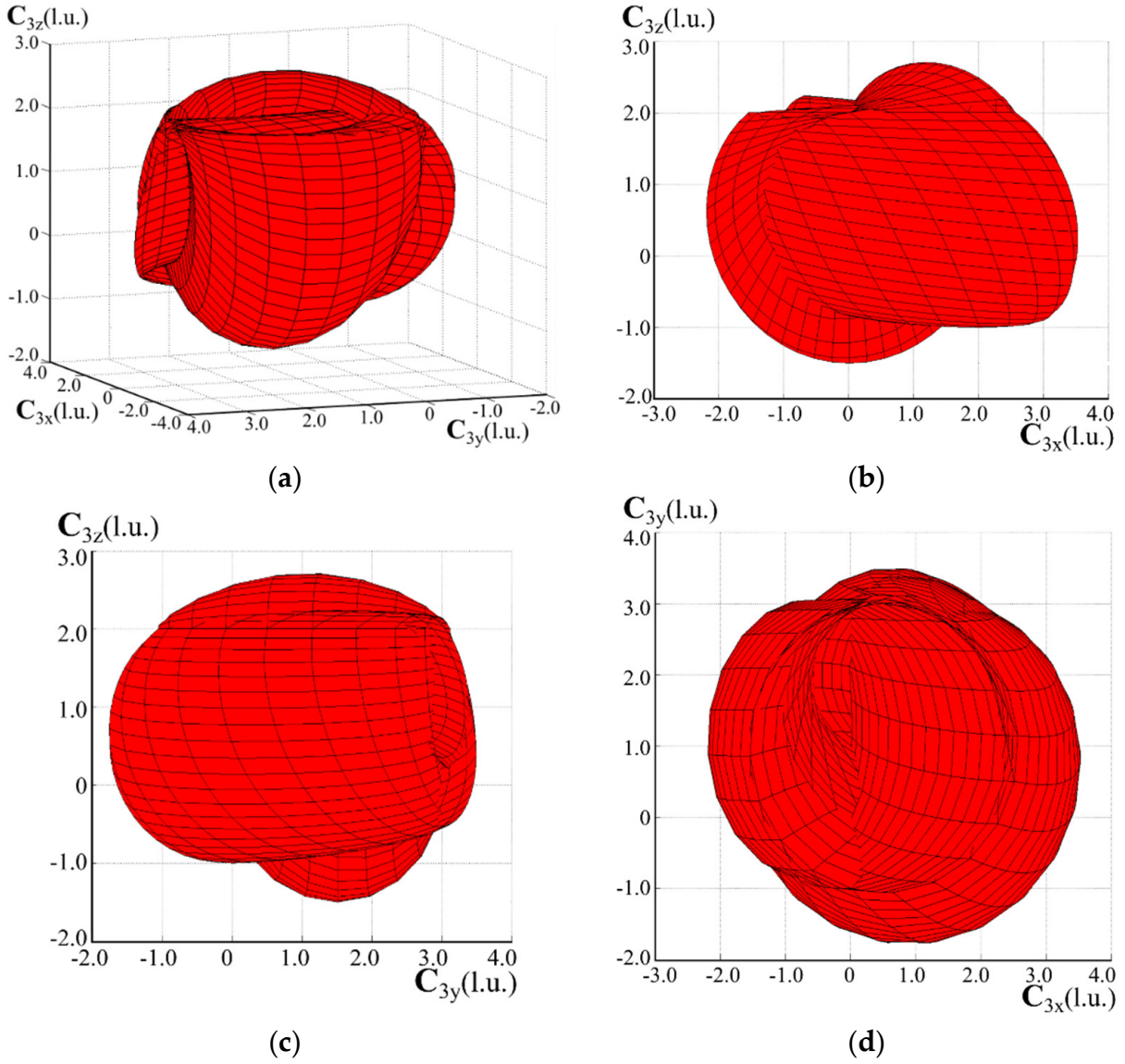

Figure 7. Volume inside which point C_3 moves while the directions of unit vectors $\mathbf{n}_i$, for i = 1, 2, 3, are modified (by keeping them mutually orthogonal) to make the platform reach the orientation shown in Figure 6 (the coordinates of point C_3 measured in $O_0x_0y_0z_0$ are reported on the axes): (**a**) 3D view, (**b**) projection onto the xz-plane, (**c**) projection onto the yz-plane, and (**d**) projection onto the xy-plane.

4. Discussion

The numerical procedure adopted to determine Figures 6 and 7 firstly considers matrix **N** as a rotation matrix, since unit vectors $\mathbf{n}_i$, for i = 1, 2, 3, must be kept mutually orthogonal, and expresses matrix **N** through the ZYZ Euler angles (ψ_1, ψ_2, ψ_3) with ψ_1, $\psi_3 \in [-\pi, \pi]$ rad and $\psi_2 \in [0, \pi]$ rad. Then, it discretizes the values of ψ_1, ψ_2, and ψ_3 by selecting a number, say k, of equally spaced values in their ranges, computes the corresponding k^3 platform poses, and keeps only those compatible with the link lengths. Eventually, the k value is increased until the shape of the determined workspace does not change; such a condition was reached for k = 40, and Figures 6 and 7 refer to k = 40. Accordingly, Figures 6 and 7 display the workspace restricted to the fully isotropic configurations, hereafter named the fully isotropic workspace.

The analysis of Figure 6 highlights that the fully isotropic orientation workspace includes an ample portion of the parallelepiped (i.e., ϕ_1, $\phi_3 \in [-\pi, \pi]$ rad and $\phi_2 \in [0, \pi]$

rad) collecting all the possible orientations the platform could assume as a free rigid body. Moreover, the sizes of the excluded regions depend on the chosen link length, which brings one to conclude that, during design, the link lengths can be sized for an assigned fully isotropic orientation workspace.

Accepting non-singular configurations with $j_n \geq j_{n,min} < 1$ and $j_{n\times m} \geq j_{n\times m,min} < 1$, where $j_{n,min}$ and $j_{n\times m,min}$ are two constant values not equal to zero, is another design choice that could be adopted to obtain the desired free-from-singularity workspace. Such an approach might also be implemented by modifying the control strategy in an already manufactured machine.

Whatever the adopted design criteria happen to be, the above case study proves that, in the family of 3-XXRRU PMs, suitable combinations of geometries and control strategies can be selected which provide good kinetostatic performance in an ample free-from-singularity workspace.

The 3-RRU structure studied in Section 3 lends itself to better illustrate the parallel-singularity conditions (i.e., Equations (10a) and (10b)) through Figures 8 and 9. Figure 8 shows two singular configurations of this structure that satisfy Equation (10a). In particular, the three unit vectors $\mathbf{n}_i$, for $i = 1, 2, 3$, are all parallel to the x_0y_0-coordinate plane with the three R-pair axes (A_i, $\mathbf{n}_i$), for $i = 1, 2, 3$, that are not coplanar in Figure 8a and are coplanar in Figure 8b. The analysis of Figure 8 clearly shows that the particular disposition of the first three R-pair axes of each limb makes platform translation possible along the z_0-coordinate axis. Differently, Figure 9 shows one singular configuration of the same structure that satisfies Equation (10b). Indeed, in such a configuration, the three unit vectors $\mathbf{n}_i \times \mathbf{m}_i$, for $i = 1, 2, 3$, are all parallel to the x_0y_0-coordinate plane. The analysis of Figure 9 clearly shows that the particular disposition of all the R-pair axes makes the platform rotation possible around the axis (C_3, $\mathbf{z}_0$).

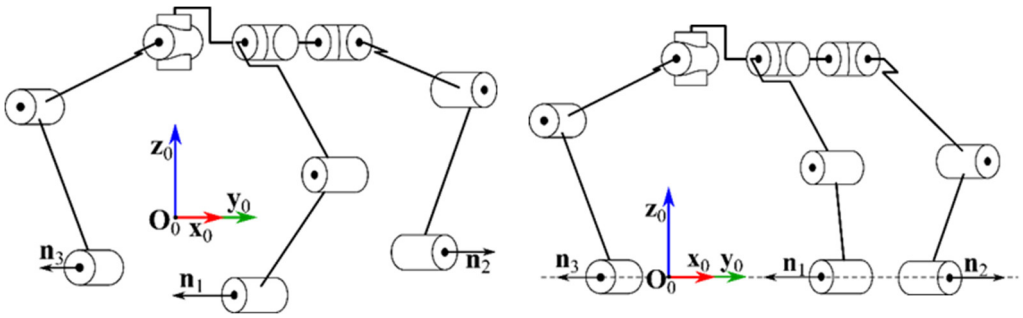

Figure 8. Two singular configurations of the 3-RRU structure of Figure 4 that satisfy Equation (10a): (**a**) the three unit vectors $\mathbf{n}_i$, for $i = 1, 2, 3$, are all parallel to the x_0y_0-coordinate plane with the three R-pair axes (A_i, $\mathbf{n}_i$), for $i = 1, 2, 3$, that are not coplanar, and (**b**) all three R-pair axes (A_i, $\mathbf{n}_i$), for $i = 1, 2, 3$, lie on the x_0y_0-coordinate plane indicated by the dashed line.

Eventually, the possible types of XX mechanisms that implement the optimal control strategy identified in Section 2 deserve a more detailed discussion. Firstly, the orientation of $\mathbf{n}_i$ can be obtained by using any parallel pointing system[8] (PPS) among the many proposed in the literature (see, for instance, Refs. [29,30]). Then, by placing a partially actuated cylindrical(C) pair[9] on the mobile platform of the PPS, with the translation that is alternatively actuated by one of the two actuators that moves the PPS platform and with

[8] A PPS is a 2-DOF PM that is able to freely orientate one line fixed to its platform by keeping one point of the line fixed to the base. They are employed in many applications like the motion of a telescope or of a parabolic antenna, etc.

[9] It is worth noting that a C-pair can be obtained by putting in series a prismatic (P) pair and an R-pair whose axis is parallel to the sliding direction of the P-pair and that such a PR chain is easy to actuate. In such a PR chain, the R-pair will be the first non-actuated R-pair of the remaining RRU chain of the XXRRU limb.

the C-pair axis that passes through the center of the spherical motion the PPS imposes to its platform, the desired translation of point A_i along the $\mathbf{n}_i$ direction can be added to the orientation of $\mathbf{n}_i$. The non-actuated rotation of the added C-pair plays the role of the first non-actuated R-pair of the remaining RRU chain of the XXRRU limb. In order to better illustrate this description, Figure 10 shows a possible XXRRU limb where the PPS is a spherical five-bar linkage[10]. Of course, the system of brakes and clutches that allows the actuation of the translation in the C-pair by means of one of the two actuators used to orientate the PPS platform needs an ad hoc design that depends on the chosen PPS.

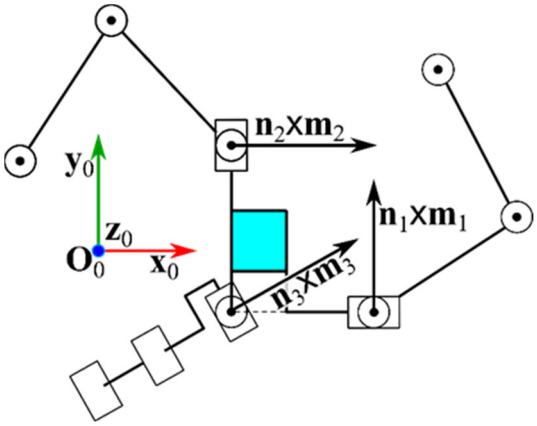

Figure 9. One singular configuration of the 3-RRU structure of Figure 4 that satisfies Equation (10b): the three unit vectors $\mathbf{n}_i \times \mathbf{m}_i$, for $i = 1, 2, 3$, are all parallel to the x_0y_0-coordinate plane.

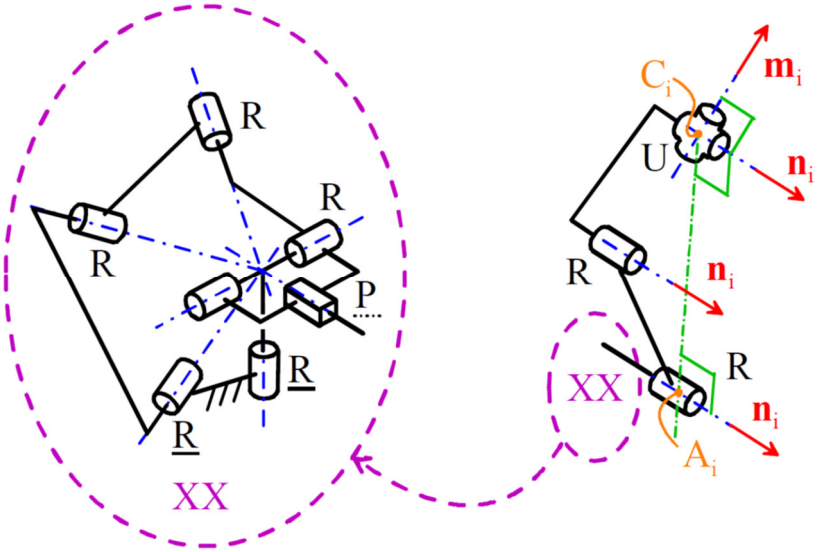

Figure 10. Example of the XXRRU limb where the PPS is a spherical five-bar linkage: the two R-pairs with a solid underscore are the two actuated pairs, adjacent to the base, that control the orientation of unit vector $\mathbf{n}_i$, whereas the P pair with a dotted underscore is the alternately actuated/locked P pair that moves point A_i along the direction of unit vector $\mathbf{n}_i$.

5. Conclusions

This study investigates the instantaneous kinematics, workspace, and kinetostatic performance of a novel family of six-DOF three-legged parallel manipulators (PMs) recently

[10] The spherical five-bar linkage is a particular PPS consisting of five binary links sequentially connected, to form a single-loop, through R-pairs whose axes share a common intersection point. This R-pair axes' arrangement guarantees that their intersection point is fixed to the frame (i.e., the links' motion is spherical) and that any line, which is fixed to a mobile link and passes through the above-mentioned intersection point, keeps that point at rest during the link motion. In Figure 10, the blue lines are the R-pair axes.

introduced by the authors in a previous publication. These PMs all share the common feature that, when their actuators are locked, they transform into 3-RRU structures and are collectively referred to as 3-XXRRU manipulators.

The examination of the instantaneous kinematics of 3-XXRRU PMs led to the derivation of a general expression for their input–output instantaneous relationship (IOR). Subsequently, the analysis of this IOR unveiled that the singularity conditions for these manipulators can be expressed in a straightforward and easily interpretable geometric manner. This insight provides valuable guidance for selecting an effective actuation system.

In combination with the static analysis of 3-XXRRU PMs, these findings led to the proposal of two dimensionless indices, ranging from 0 to 1, which measure the proximity of a non-singular configuration to the nearest parallel singularity. These indices can be employed in the dimensional synthesis of these PMs. Utilizing these indices, a suitable control strategy has been devised to maintain manipulator isotropy, particularly concerning the resultant force of external forces applied to the platform.

Lastly, a specific platform geometry has been introduced, enabling the attainment of an ample fully isotropic workspace.

6. Patents

Simas H., Simoni R., Meneghini L., Di Gregorio R.: Manipulador paralelo 3XXRRU com três pernas e seis graus de liberdade com volume de trabalho ampliado. 2023; Brazil Patent Application No. BR 10 2023 013289 8; Instituto Nacional da Propriedade Industrial -Brazil.

Author Contributions: Conceptualization, H.S., R.D.G. and R.S.; methodology, H.S., R.D.G. and R.S.; software, H.S.; validation, H.S., R.D.G. and R.S.; formal analysis, H.S., R.D.G. and R.S.; investigation, H.S., R.D.G. and R.S.; writing—original draft preparation, H.S., R.D.G. and R.S.; writing—review and editing, R.D.G.; visualization, R.S.; supervision, R.D.G.; project administration, H.S.; funding acquisition, H.S., R.D.G. and R.S. All authors have read and agreed to the published version of the manuscript.

Funding: This research was developed at the Laboratory of Mechatronics and Virtual Prototyping (LaMaViP) of Ferrara Technopole, supported by the UNIFE FIRD2023 fund, in partnership with the Laboratory of Applied Robotics of Federal University of Santa Catarina, supported by CNPq—*Conselho Nacional de Desenvolvimento Científico e Tecnológico* (National Council for Scientific and Technological Development) Project 307249/2021-2, Brazil.

Institutional Review Board Statement: Not applicable.

Data Availability Statement: This work does not use experimental data. The data necessary to replicate the computations illustrated in the paper are included in the text of the paper.

Conflicts of Interest: The authors declare no conflict of interest.

References

1. Merlet, J.-P. *Parallel Robots*; Springer: Berlin/Heidelberg, Germany, 2000; ISBN 978-1-4020-0385-1.
2. Tsai, L.-W. *Mechanism Design: Enumeration of Kinematic Structures According to Function*; CRC Press: London, UK, 2001; ISBN 978-0-8493-0901-4.
3. Tsai, L.-W. *Robot Analysis: The Mechanics of Serial and Parallel Manipulators*; John Wiley & Sons: New York, NY, USA, 1999; ISBN 978-0-4713-2593-2.
4. Meng, J.; Liu, G.; Li, Z. A geometric theory for analysis and synthesis of sub-6 DoF parallel manipulators. *IEEE Trans. Robot.* **2007**, *23*, 625–649. [CrossRef]
5. Lin, R.; Guo, W.; Gao, F. Type Synthesis of a Family of Novel Four, Five, and Six Degrees-of-Freedom Sea Lion Ball Mechanisms With Three Limbs. *ASME J. Mech. Robot.* **2016**, *8*, 021023. [CrossRef]
6. Cleary, K.; Brooks, T. Kinematic analysis of a novel 6-DOF parallel manipulator. In Proceedings of the 1993 IEEE International Conference on Robotics and Automation, Atlanta, GA, USA, 2–6 May 1993; Volume 1, pp. 708–713. [CrossRef]
7. Jin, Y.; Chen, I.-M.; Yang, G. Kinematic design of a family of 6-DOF partially decoupled parallel manipulators. *Mech. Mach. Theory* **2009**, *44*, 912–922. [CrossRef]
8. Coppola, G.; Zhang, D.; Liu, K. A 6-DOF reconfigurable hybrid parallel manipulator. *Robot. Comput. Integr. Manuf.* **2014**, *30*, 99–106. [CrossRef]

9. Monsarrat, B.; Gosselin, C.M. Workspace analysis and optimal design of a 3-leg 6-DOF parallel platform mechanism. *IEEE Trans. Robot. Autom.* **2003**, *19*, 954–966. [CrossRef]
10. Angeles, J.; Yang, G.; Chen, I.-M. Singularity analysis of three-legged, six-dof platform manipulators with URS legs. *IEEE/ASME Trans. Mechatron.* **2003**, *8*, 469–475. [CrossRef]
11. Yang, Z.; Zhang, D. Novel Design of a 3-RRUU 6-DOF Parallel Manipulator. *IOP Conf. Ser. Mater. Sci. Eng.* **2019**, *491*, 012006. [CrossRef]
12. Fu, J.; Gao, F. Optimal design of a 3-leg 6-DOF parallel manipulator for a specific workspace. *Chin. J. Mech. Eng.* **2016**, *29*, 659–668. [CrossRef]
13. Seward, N.; Bonev, I.A. A new 6-DOF parallel robot with simple kinematic model. In Proceedings of the 2014 IEEE International Conference on Robotics and Automation (ICRA), Hong Kong, China, 31 May–7 June 2014; pp. 4061–4066. [CrossRef]
14. Lu, Y.; Wang, P.; Hou, Z.; Hu, B.; Sui, C.; Han, J. Kinetostatic analysis of a novel 6-DoF 3UPS parallel manipulator with multi-fingers. *Mech. Mach. Theory* **2014**, *78*, 36–50. [CrossRef]
15. Simas, H.; Meneghini, L.; Di Gregorio, R.; Simoni, R. Position Analysis of a Novel Family of three-legged 6-DOF Parallel Manipulators of type 3-XXRRU. In *Advances in Mechanism and Machine Science: Proceedings of the 16th IFToMM World Congress 2023 [WC2023], Tokyo, Japan, 5–10 November 2023*; Okada, M., Ed.; Paper No.: 147; Springer: Cham, Switzerland, 2023.
16. Gosselin, C.M.; Angeles, J. Singularity analysis of closed-loop kinematic chains. *IEEE Trans. Robot. Automat.* **1990**, *6*, 281–290. [CrossRef]
17. Ma, O.; Angeles, J. Architecture singularities of platform manipulators. In Proceedings of the 1991 IEEE International Conference on Robotics and Automation, Sacramento, CA, USA, 9–11 April 1991; pp. 1542–1547.
18. Zlatanov, D.; Fenton, R.G.; Benhabib, B. A unifying framework for classification and interpretation of mechanism singularities. *ASME J. Mech. Des.* **1995**, *117*, 566–572. [CrossRef]
19. Zlatanov, D.; Bonev, I.A.; Gosselin, C.M. Constraint Singularities as C-Space Singularities. In Proceedings of the 8th International Symposium on Advances in Robot Kinematics (ARK 2002), Caldes de Malavella, Spain, 24–28 June 2002.
20. Zlatanov, D.; Bonev, I.A.; Gosselin, C.M. Constraint singularities of parallel mechanisms. In Proceedings of the 2002 IEEE International Conference On Robotics & Automation, Washington, DC, USA, 11–15 May 2002; pp. 496–502.
21. Hunt, K.H. *Kinematic Geometry of Mechanisms*; Oxford University Press: Oxford, UK, 1978.
22. Davidson, J.K.; Hunt, K.H. *Robots and Screw Theory: Applications of Kinematics and Statics to Robotics*; Oxford University Press: Oxford, UK, 2005.
23. Uicker, J., Jr.; Pennock, G.; Shigley, J. *Theory of Machines and Mechanisms*, 5th ed.; Oxforf University Press: Oxford, UK, 2016.
24. Kim, H.S.; Tsai, L.-W. Evaluation of a Cartesian parallel manipulator. In *Advances in Robot Kinematics*; Lenarcic, J., Thomas, F., Eds.; Kluwer Academic Publishers: London, UK, 2002; pp. 21–28.
25. Kim, H.S.; Tsai, L.-W. Design Optimization of a Cartesian Parallel Manipulator. *ASME J. Mech. Des.* **2003**, *125*, 43–51. [CrossRef]
26. Silvester, J.R. Determinants of block matrices. *Math. Gaz.* **2000**, *84*, 460–467. [CrossRef]
27. Sothanaphan, N. Determinants of block matrices with noncommuting blocks. *Linear Algebra Its Appl.* **2017**, *512*, 202–218. [CrossRef]
28. Angeles, J. *Fundamentals of Robotic Mechanical Systems*, 4th ed.; Springer: Cham, Switzerland, 2014; ISBN 978-3-319-30762-6.
29. Hervé, J.M. Uncoupled actuation of pan-tilt wrists. *IEEE Trans. Robot.* **2006**, *22*, 56–64. [CrossRef]
30. Li, Q.; Hervé, J.M.; Ye, W. *Geometric Method for Type Synthesis of Parallel Manipulators*; Springer: Singapore, 2020; pp. 223–238. ISBN 978-981-13-8754-8. [CrossRef]